ONCOIMMUNOLOGY
2023, VOL. 12, NO. 1, 2240678
https://doi.org/10.1080/2162402X.2023.2240678

Taylor & Francis
Taylor & Francis Group

ORIGINAL RESEARCH

OPEN ACCESS Check for updates

The yes-associated protein (YAP) is associated with resistance to anti-GD2 immunotherapy in neuroblastoma through downregulation of *ST8SIA1*

Adeiye A. Pilgrim[a], Hunter C. Jonus[a], Andrew Ho[a], Anna C. Cole[b,c], Jenny Shim[a,d], and Kelly C. Goldsmith[a,d]

[a]Department of Pediatrics, Emory University School of Medicine, Atlanta, GA, USA; [b]Division of Surgical Oncology, Department of Surgery, Emory University, Atlanta, GA, USA; [c]Department of Microbiology and Immunology, Winship Cancer Institute, Emory University, Atlanta, GA, USA; [d]Aflac Cancer and Blood Disorders Center, The Children's Healthcare of Atlanta, Atlanta, Georgia

ABSTRACT

Pediatric patients with high-risk neuroblastoma often relapse with chemotherapy-resistant, incurable disease. Relapsed neuroblastomas harbor chemo-resistant mesenchymal tumor cells and increased expression/activity of the transcriptional co-regulator, the Yes-Associated Protein (YAP). Patients with relapsed neuroblastoma are often treated with immunotherapy such as the anti-GD2 antibody, dinutuximab, in combination with chemotherapy. We have previously shown that YAP mediates both chemotherapy and MEK inhibitor resistance in relapsed *RAS* mutated neuroblastoma and so posited that YAP might also be involved in anti-GD2 antibody resistance. We now show that YAP genetic inhibition significantly enhances sensitivity of mesenchymal neuroblastomas to dinutuximab and gamma delta (γδ) T cells both *in vitro* and *in vivo*. Mechanistically, YAP inhibition induces increased GD2 cell surface expression through upregulation of *ST8SIA1*, the gene encoding GD3 synthase and the rate-limiting enzyme in GD2 biosynthesis. The mechanism of *ST8SIA1* suppression by YAP is independent of *PRRX1* expression, a mesenchymal master transcription factor, suggesting YAP may be the downstream effector of mesenchymal GD2 resistance. These results therefore identify YAP as a therapeutic target to augment GD2 immunotherapy responses in patients with neuroblastoma.

ARTICLE HISTORY
Received 2 April 2023
Revised 21 July 2023
Accepted 21 July 2023

KEYWORDS
chemoimmunotherapy; dinutuximab; GD2; neuroblastoma; relapse; YAP

Introduction

Clinical outcomes for children with the extracranial solid tumor neuroblastoma remain unsatisfactory. Following intensive multimodal treatment, greater than half of patients with high-risk neuroblastoma relapse with a substantially reduced chance for cure.[1–4] To improve outcomes for these patients requires a greater understanding and therapeutic targeting of pathways regulating disease recurrence. Relapsed neuroblastoma is characterized by an increased frequency of genomic alterations that activate the RAS-MAPK pathway, such as activating mutations in *ALK*, *KRAS*, *NRAS*, *HRAS*, *PTPN11* and inactivating mutations of *NF1 and PTPN14*.[5–7] In its active state, PTPN14 inhibits the nuclear localization of the Yes-associated protein (YAP) to prevent YAP-mediated transcription.[6–10] Accordingly, the same genome-wide association studies of relapsed neuroblastomas also identified a significant increase in YAP transcriptional activity, suggesting a potential role for YAP in recurrent neuroblastoma.[10]

YAP is a transcriptional co-regulator that primarily binds to TEAD family transcription factors.[11,12] YAP and TEAD transcriptionally activate or repress downstream target genes, contributing to cell proliferation, self-renewal and survival in many cancers, including neuroblastoma.[13,14] YAP is highly expressed in neuroblastoma cells that demonstrate an undifferentiated mesenchymal phenotype, which is characteristically chemotherapy resistant.[10,15] Using paired high-risk neuroblastoma tumors derived from the same patient at diagnosis and at tumor recurrence following chemotherapy, we have previously shown increased YAP expression and transcriptional activity at relapse.[16] Genetic inhibition of YAP delayed tumor growth and sensitized *NRAS*-mutated neuroblastoma xenografts to cytotoxic chemotherapy and MEK inhibitor treatment *in vivo*, yet failed to have the same effects *in vitro*, suggesting YAP plays a crucial role driving therapy resistance within the solid tumor microenvironment (TME).[16,17] RNA sequencing of neuroblastomas with and without YAP genetic knockdown revealed that YAP suppresses the BH3 pro-death gene, *HRK*, to attenuate chemotherapy and MEK inhibitor responses *in vivo*.[16] Therefore, YAP upregulation following chemotherapy and relapse promotes therapy resistance in high-risk neuroblastoma through transcriptional repression of genes that play a role in the TME.

A common approach to treating patients with chemotherapy resistant, relapsed neuroblastoma uses immunotherapies targeting neuroblastoma-specific tumor antigens. The glycosphingolipid GD2 is expressed on the surface of neuroblastomas,[18–21] and the introduction of humanized monoclonal antibodies targeting GD2 (i.e. dinutuximab) significantly improved survival for newly diagnosed patients with high-risk disease.[22,23] Anti-GD2 antibodies have also been combined with cytotoxic chemotherapy ("chemoimmunotherapy"), which demonstrated impressive response rates for

CONTACT Kelly C. Goldsmith kgoldsm@emory.edu Department of Pediatrics, Emory University School of Medicine, Atlanta, GA, USA
Supplemental data for this article can be accessed online at https://doi.org/10.1080/2162402X.2023.2240678

relapsed neuroblastoma and resulted in GD2 chemoimmunotherapy becoming the most widely used salvage therapy for patients with refractory or relapsed disease.[3,24] Unfortunately, not all patients respond to GD2-targeting immunotherapies and robust biomarkers of response are so far lacking, leaving many to suffer toxicities with no clinical antitumor benefit.[23,25,26]

Resistance to immunotherapy can be caused by lack of expression or downregulation of the cell surface target of interest.[27] Indeed, GD2 can become downregulated following therapy and neuroblastoma recurrence.[28–30] Recent studies also suggest that mesenchymal neuroblastomas resist GD2-targeted therapies via inhibition of GD2 synthesis, yet the role for YAP, a canonical mesenchymal marker, has not been explored.[31] Given the increased expression and activity of YAP in relapsed neuroblastoma, and its role in mediating cytotoxic and targeted therapy resistance, we posited that YAP plays a role in GD2 immunotherapy response. Here, we demonstrate for the first time that YAP genetic inhibition sensitizes neuroblastomas to anti-GD2 antibody *in vitro* and *in vivo*. We further show that YAP transcriptionally suppresses *ST8SIA1* that encodes GD3 synthase, the rate-limiting enzyme for GD2 synthesis, supporting that YAP inhibition can be leveraged therapeutically to enhance patient responses to immunotherapeutic approaches targeting GD2.

Materials and methods

Cell culture

Human-derived neuroblastoma cell lines, CHLA-255, NLF, and SK-N-AS were cultured in RPMI supplemented with 10% fetal bovine serum (FBS) and 1% penicillin/streptomycin at 37°C, 5% CO_2. Cell lines were routinely STR genotyped and resulting identities were confirmed to match the COG cell line database (cccells.org). Cells were also verified to be free of *Mycoplasma* contamination using the MycoAlert contamination kit (Lonza).

Generation of stably transduced cell lines

YAP was stably inhibited genetically through short hairpin RNA (shRNA) as previously described.[16] *ST8SIA1* was genetically inhibited stably in shYAP SK-N-AS cells as previously published using two independent constructs expressing *ST8SIA1*-targeting shRNAs (Genecopoeia LVRU6H-b (shGD3S–1) and LVRU6H-c (shGD3S–2)) and a hygromycin selection marker.[16] The equivalent non-targeting control vectors were transduced appropriately (Sigma SHC016 (control) and Genecopoeia CSI-neg-LVRU6H (LV control)). Cells with successful lentiviral transduction were selected with 2ug/mL puromycin (YAP constructs) and 150ug/mL hygromycin (ST8SIA1 constructs).

Western blot analysis

Neuroblastoma cells were harvested with versene (ThermoFisher Scientific) and lysed in CHAPS buffer (10 mM HEPES, 150 mM NaCl, 2% CHAPS) supplemented with 1% PMSF, 1% Protease Inhibitor Cocktail (Roche), and 4% sodium orthovanadate on ice for 2 hours. Debris was cleared from resulting lysates by centrifugation at 8000 rcf for 15 mins. Protein concentration was quantified by Bradford assay. 25 ug of total protein was loaded on 4–12% NuPage Bis-Tris gels (ThermoFisher Scientific) and electrophoresed at 200 V for 35 mins. Separated proteins were transferred onto polyvinylidene difluoride (PVDF) membranes at 30 V for 90 minutes. Primary antibodies were diluted in 5% blocking buffer (Bio-Rad) in tris-buffered saline with Tween 20 (TBST) overnight and secondary anti-rabbit or anti-mouse HRP for 2 hours as appropriate. Membranes were imaged by chemiluminescence using Pierce ECL substrate (Thermofisher Scientific). See Supplemental Table S1 for antibody information.

Gamma delta (γδ) T cell expansion

γδ T cells were expanded under our 12-day protocol as previously described with αβ T cell depletion on day 6 of culture from healthy donor peripheral blood mononuclear cells.[32] The expanded γδ T cell population was profiled by flow cytometry with antibodies: CD3-BV421, CD56-APC-R700, CD16-BV480, and αβ-TCR-PE or γδ-TCR-PE and used between days 12 and 14 in the cytotoxicity assays described below.[32] See Supplemental Table S2 for antibody information.

Cytotoxicity assays

Bioluminescence-based

GFP-luciferase-tagged neuroblastoma cell lines were plated at 34,000/well in RPMI supplemented with 10% heat-inactivated FBS in 96-well plates and allowed to adhere overnight. The following day, γδ T cells were added at increasing effector-to-target (E:T) ratios (0:1, 1:1, and 5:1), with and without 5ug/mL dinutuximab. Co-cultures were incubated for 4 hours prior to the addition of luciferin (75ug/mL, PerkinElmer) for detection of viable target (NB) cells. Luminescent signal was detected using the Promega GloMax™-Multi Detection System. The calculation of death was performed using the following formula: %specific lysis = 100 × (spontaneous death RLU – test RLU)/(spontaneous death RLU – maximal killing RLU) where RLU is an abbreviation for relative luminescence units.

Flow cytometry-based

Neuroblastoma cells were labeled with Violet Proliferation Dye 450 (VPD450, BD Biosciences) and plated in RPMI supplemented with 10% heat-inactivated FBS at 200,000 cells/well in 24-well plates and allowed to adhere overnight. The following day, fresh γδ T cells from expansion day 12 or 14 were added to neuroblastoma cells for co-culture at increasing E:T ratios (γδ T cells-to-neuroblastoma cells) (0:1, 1:1 and 5:1) in the presence and absence of dinutuximab (5 ug/mL, United Therapeutics). Cells were incubated together for 4 hours and then harvested with accutase (GeminiBio). Cells were washed with PBS and resuspended in Annexin V binding buffer (Biolegend), stained with Annexin V-APC antibody (Biolegend) and analyzed immediately on the Aurora Cytek spectral flow cytometer. Prior to acquisition, BD Via-Probe cell viability solution (BD Biosciences) was added to the cell suspension. Unmixing of flow cytometry data

was performed at the cytometer with further data analysis and gating performed using FlowJo v10.8.1 (FlowJo, LLC) software. See Supplemental Figure S1 for gating strategy.

Detection of human IFNγ by enzyme-linked immunosorbent assay (ELISA)

Human IFNγ was detected using a commercial kit (Biolegend). Supernatants were harvested from cytotoxicity assays in which SK-N-AS control, shYAP1 and shYAP2 neuroblastoma cells were co-cultured with γδ T cells at E:T ratios of 0:1, 1:1, and 5:1 for 4 hours. Briefly, supernatants were centrifuged to remove cell debris. IFNγ standards were generated by reconstituting recombinant IFNγ (Biolegend) in sterile deionized water. Concentrations of IFNγ in samples and standards were determined per manufacturer's instructions. The BioTek Synergy Mx Microplate reader was used to read absorbance at 450 nm.

Flow cytometry

GD2 staining of neuroblastoma cell lines and xenografts

Cells were harvested with versene (Gibco), washed in phosphate-buffered saline (PBS), followed by resuspension in FACs buffer (PBS, 10% FBS, 0.1% sodium azide, 5 mM EDTA), and then stained with the live-dead stain, fixable viability stain 780 (BD Biosciences), by incubation at room temperature protected from light. Cells were then washed and stained with Isotype-BV421/GD2-BV421 only for *in vitro* GD2 characterization and CD45-PerCP-Cy5.5, CD56-PE, CD81-FITC, Isotype-BV421 /GD2-BV421, for *in vivo* GD2 characterization at room temperature, washed twice in FACs buffer and resuspended for data acquisition on the Cytek Aurora 5-laser spectral flow cytometer. Negative controls were fluorescence minus one (FMO) controls for NBx28r and SKNAS CDX, unstained for NBx14r, NBx27, NBx 34r (due to lack of tissue availability). All neuroblastoma patient-derived xenografts (PDXs) were passage 2 or less. Data were analyzed using FlowJo version 10.9.0. See gating strategy (*in vitro*) in Supplemental Figure S2. See Supplemental Table S3 for antibody information.

Determination of γδ T cell activation state (CD107a staining)

Neuroblastoma cells (SK-N-AS control, SK-N-AS shYAP1, and shYAP2) were co-cultured with γδ T cells at an E:T ratio of 1:1 as described in the flow cytometry-based cytotoxicity assay protocol above. CD107a-PE Cy7 antibody was added to each well 30 minutes after the cytotoxic assay was started. GolgiStop (BD Biosciences) was added one hour later at a final concentration of 0.7uL/mL. At the endpoint, γδ T cells were harvested and stained with CD3-BV421, CD56-APC-R700, and γδ TCR-PE, washed twice in FACs buffer and resuspended for data acquisition on the Cytek Aurora 5-laser spectral flow cytometer. See Supplemental Table S2 for antibody information. Data were analyzed using FlowJo version 10.8.1.

Extensive characterization of γδ T cells pre- and post-cytotoxicity assay

Neuroblastoma cells (SK-N-AS control, SK-N-AS shYAP1, and shYAP2) and γδ T cells were co-cultured at a 1:0 or 1:1 E:T ratio for 24 hours. The γδ T cells were harvested at 24 hours and profiled using our previously published extensive characterization panel.[32] See Supplemental Table S4 for antibody information.

RT-qPCR

RNA was extracted from neuroblastoma cell lines using the TRIzol (Ambion)-chloroform (Millipore Sigma) extraction method and quantified using a NanoDrop 2000 (Thermo Scientific). cDNA was prepared from 2ug RNA by using the high-capacity cDNA reverse transcription kit (Applied Biosystems) per manufacturer's protocol. For real-time qPCR, SYBR green reagent (Applied Biosystems) was used with the primers listed in Supplemental Table S5. Gene expression was normalized to *GAPDH* and *HPRT* using the CFX96 Touch Real-Time PCR Detection System software (Bio-Rad).

Mouse xenograft in vivo studies

All animal studies were conducted in accordance with policies set forth by the Emory University Institutional Animal Care and Use Committee (IACUC). Our protocol was approved by the Emory IACUC (PROTO201700089). Euthanasia was performed by asphyxiation with CO_2 and cervical dislocation. 4×10^6 SK-N-AS cells were combined at a 1:1 ratio (by volume) with Matrigel (Corning) and injected subcutaneously into the flank of 4–6-week-old female and male NOD-*scid* IL2Rgamma^{null} (NSG) mice (The Jackson Laboratory). Tumor volume was calculated using the formula: length x width x height x p/6. When tumors grew to a volume of 100–200 mm^3, mice were randomized to the treatment groups. Mice receiving the full regimen were treated on days 1, 4, 7 and 10 with 75 mg/kg cyclophosphamide (McKesson) intraperitoneally; on days 2, 8, and 14 with 100ug dinutuximab intravenously; on days 3, 6, 9, 12, 15, and 18 with 2.5×10^6 γδ T cells (expanded from healthy human blood as described above) intratumorally. Mice were sacrificed when tumor burden reached IACUC-prescribed limit based on tumor volume (1500 mm^3) and physical burden. Tumors were harvested and mechanically dissociated to extract RNA and protein to perform RT-qPCR, western blots, and flow cytometry as described above.

Statistical analyses

GraphPad Prism v9.4.1 was used to perform all statistical analyses. For pairwise comparisons throughout, unpaired t-tests with Welch's correction were calculated. Kaplan–Meier survival plots were generated for *in vivo* investigations, and log rank test was performed to determine statistical significance.

Results

Neuroblastoma cell lines that express high YAP and low GD2 are resistant to dinutuximab and gamma delta (γδ) T cell treatment in vitro

Given the increased expression and activity of YAP in relapsed neuroblastoma and its influence on chemotherapy response, we sought to determine if YAP might also play a role in GD2

immunotherapy response. We first evaluated YAP and GD2 expression in three neuroblastoma cell lines: SK-N-AS, NLF, and CHLA-255. YAP protein expression was high in SK-N-AS (MYCN non-amplified) and NLF (MYCN amplified) while undetectable in CHLA-255 (MYCN amplified) (Figure 1A). GD2 cell surface expression was conversely low in neuroblastoma cells with high YAP expression, SK-N-AS and NLF, and high in CHLA-255 that expresses no YAP (Figure 1B). Gamma delta (γδ) T cells are an innate effector immune cell subset that can regulate antibody-dependent cell-mediated cytotoxicity (ADCC). γδ T cells have been shown by our group to synergize with dinutuximab against neuroblastoma models both *in vitro* and *in vivo*.[32,33] We therefore used *ex vivo* expanded γδ T cells as the immune effectors in combination with dinutuximab in these investigations. Agnostic of MYCN amplification state, $GD2^{low}/YAP^{high}$ cell lines, SK-N-AS and NLF were resistant to γδ T cell-induced specific lysis with and without dinutuximab treatment (Figure 1C). Contrastingly, γδ T cells alone induced specific lysis of $GD2^{high}/YAP^{low}$ cell line CHLA-255, with γδ T cell-mediated specific lysis significantly enhanced by the addition of dinutuximab at both 1:1 and 5:1 effector: target (E:T) ratios (Figure 1C).

YAP inhibition sensitizes neuroblastomas to dinutuximab and γδ T cells in vitro and in vivo through upregulation of GD2 cell surface expression

Based on the inverse correlation of YAP and GD2 expression in neuroblastomas and differential dinutuximab responses, we evaluated the role for YAP in dinutuximab response through genetic knockdown. Using $GD2^{low}$ and dinutuximab-resistant SK-N-AS that harbors an activating *NRAS Q61K* mutation, we generated stable YAP knockdown models using short hairpin (sh)RNA. Western blot analysis confirmed genetic inhibition of YAP in SK-N-AS cells selected to stably express YAP-silencing shRNA (shYAP1, shYAP2) compared to a non-targeting, scrambled control (Figure 2A). Increased cytotoxicity of γδ T cells alone was observed in SK-N-AS shYAP1 and shYAP2 cells at an E:T ratio of 5:1 compared to SK-N-AS control (Figure 2B). The addition of dinutuximab in the coculture further augmented cytotoxicity of YAP-inhibited SK-N-AS by the γδ T cells (Figure 2B).

To determine the mechanism of increased sensitivity of YAP-inhibited SK-N-AS to γδ T cells both alone and in combination with dinutuximab, we first evaluated for changes in the intrinsic killing mechanisms of γδ T cells imparted by YAP knockdown in the tumor.[34] We performed flow cytometric analysis of CD107a, a cell surface marker of early degranulation used as a surrogate for γδ T cell activation.[35–37] No detectable differences in early degranulation were observed between γδ T cells co-cultured with SK-N-AS control or $SK\text{-}N\text{-}AS^{shYAP1}$ cells ± dinutuximab (**Supplemental Figure S3**). Immunophenotyping of expanded γδ T cells before and after the 24-hour co-culture with SK-N-AS control, SK-N-AS shYAP1, or SK-N-AS shYAP2 cells showed no differences or changes in γδ T cell surface expression of common markers of activation (DNAM1, NKG2D), inhibition (KIR2DL1), or exhaustion (PD1, TIM3, CTLA4, TIGIT) (**Supplemental Figure S4**).[32] γδ T lymphocytes harbor innate receptors that recognize and bind to stress ligands on the tumor cell surface, leading to T cell activation. In addition, they express FASL that binds to death receptors expressed on tumor cells, leading to perforin and granzyme release.[38,39] To elucidate whether the mechanism of increased death of SK-N-AS shYAP cells is due to changes in tumor cell surface markers or death receptors, we assessed the expression of NKG2D receptor ligands (MICA, MICB, and ULBP1/2/5/6), as well as death receptors (TRAIL-R1/2, CD95/FAS) and DNAM1 ligands (CD112/Nectin-2 and CD155/PVR). These markers did not change with YAP knockdown in SK-N-AS (**Supplemental Figure S5**).

In response to major histocompatibility complex (MHC)-independent activation by tumor cells, γδ T cells can produce

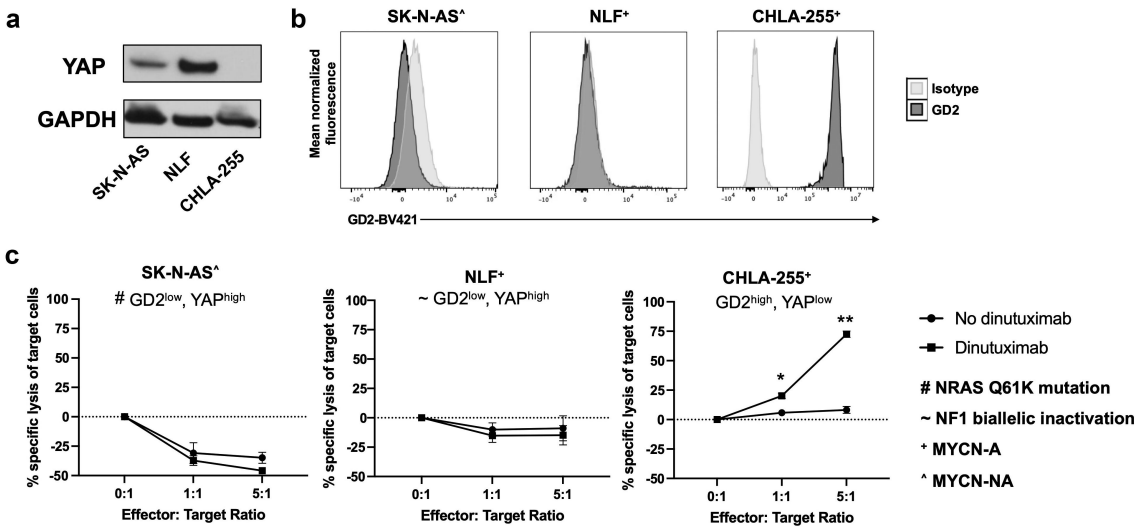

Figure 1. YAP expression is high in neuroblastoma cell lines that are resistant to anti-GD2/γδ T cell immunotherapy. A, Western blot of YAP expression in the neuroblastoma cell lines, SK-N-AS, NLF, and CHLA-255. GAPDH is the loading control. B, Mean normalized fluorescence of GD2 cell surface expression by flow cytometry in SK-N-AS, NLF, and CHLA-255. C, Percentage specific lysis after 4-hour cytotoxicity assays between γδ T cells (effector) and the neuroblastoma cell lines (target), CHLA-255, NLF and SK-N-AS at effector: target (E:T) ratios of 0:1, 1:1, and 5:1 with or without the addition of the anti-GD2 monoclonal antibody, dinutuximab. For CHLA-255, 1:1, $*p = 0.0235$, 5:1, $**p = 0.0072$. All other differences are not statistically significant.

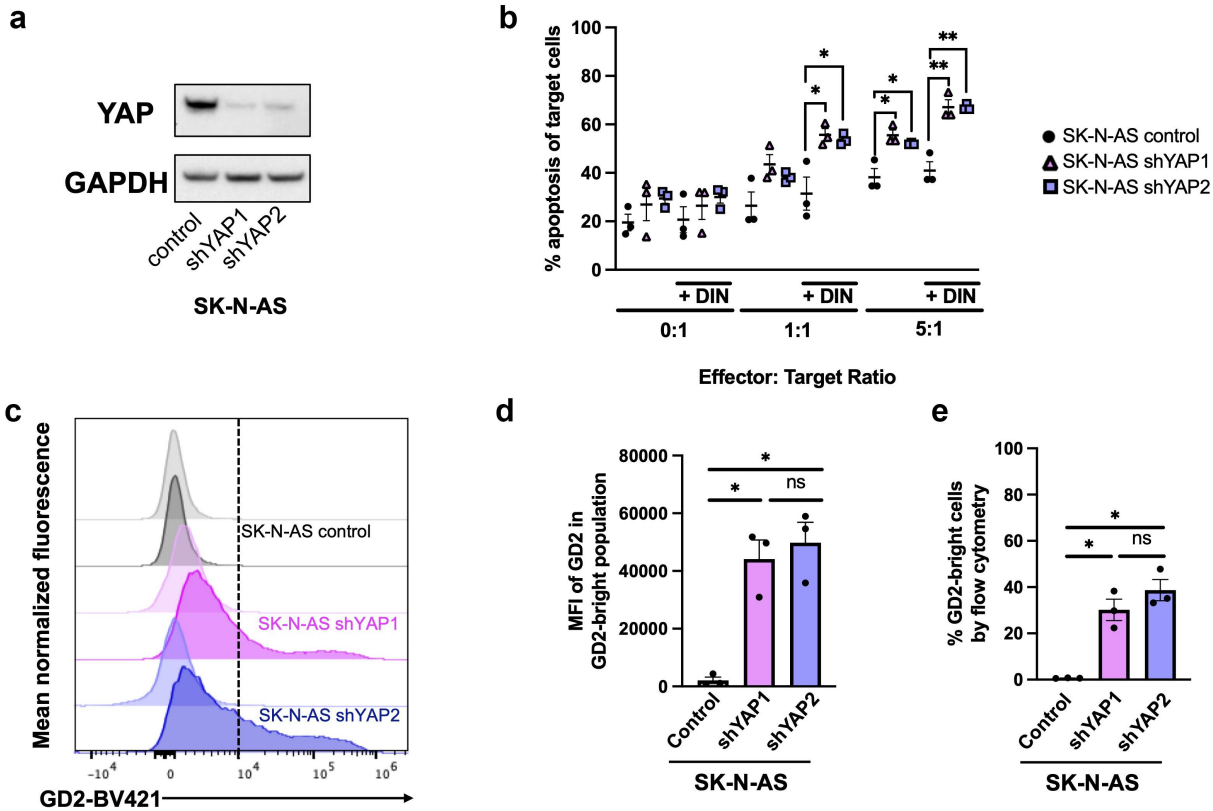

Figure 2. Genetic inhibition of YAP increases *in vitro* response to anti-GD2/γδ T cell immunotherapy with corresponding upregulation of GD2 surface expression in SK-N-AS. A, Western blot of YAP expression in control- (SK-N-AS control) and shYAP-transduced cells (SK-N-AS shYAP1 and shYAP2). GAPDH is the loading control. B, Percentage apoptosis of neuroblastoma target cells, SK-N-AS control, shYAP1 and shYAP2 when co-cultured for 4 hours with γδ T cells, with (+ DIN) and without dinutuximab, 1:1 ±DIN: control vs shYAP1, $*p = 0.0292$, control vs shYAP2, $*p = 0.0327$; 5:1: control vs shYAP1, $*p = 0.0146$, control vs shYAP2, $*p = 0.0185$; 5:1 ±DIN: control vs shYAP1, $**p = 0.0054$, control vs shYAP2, $**p = 0.0022$; Data represent mean ± standard error of $n = 3$ independent experiments with two technical replicates per condition, student's T-test with Welch's correction. All other comparisons were not significant. C, Representative graph showing mean normalized fluorescence of GD2 cell surface expression by flow cytometry in SK-N-AS control, shYAP1 and shYAP2 cell lines. Lighter colors indicate isotype controls and darker colors indicate GD2-BV421 staining. The dotted line demarcates the GD2-bright population which was quantified in D and E. D, Quantification of median fluorescence intensity (MFI) of the GD2-bright population in SK-N-AS control, shYAP1 and shYAP2 cell lines: SK-N-AS control vs shYAP1: $*p = 0.0215$, SK-N-AS control vs shYAP2: $*p = 0.0193$. Data represent mean ± standard error of $n = 3$ independent experiments. E, Percentage of GD2-bright cells by flow cytometry in SK-N-AS control, shYAP1 and shYAP2 cell lines: SK-N-AS control vs shYAP1: $*p = 0.0233$; SK-N-AS control vs shYAP2: $*p = 0.0142$. Data represent mean ± standard error of $n = 3$ independent experiments.

IFNγ.[40] IFNγ can induce apoptosis in tumor cells.[41] We therefore examined IFNγ production when γδ T cells were co-cultured with SK-N-AS shYAP or control cell lines with or without dinutuximab. In the absence of dinutuximab, we observed no difference in IFNγ concentrations when γδ T cells were co-cultured with SK-N-AS control, shYAP1 and shYAP2 cells (**Supplemental Figure S6A**). However, in the presence of dinutuximab, a statistically significant increase in IFNγ release was observed in the shYAP1 and shYAP2 co-cultures compared to control **(Supplemental Figure S6B)**, corresponding with the increased cytotoxicity observed in the shYAP cells exposed to dinutuximab and γδ T cells at 1:1 and 5:1 (Figure 2B).

The presence of antigen or changes in antigen density at the cell surface are essential determinants of response to therapies that depend on ADCC.[42] Given that intrinsic killing properties of γδ T cells are not significantly changed by differences in tumor YAP expression, we focused our attention on GD2 surface expression and its potential contribution to augment dinutuximab/γδ T cell combination effects. Wild-type SK-N-AS expresses low levels of GD2 on the cell surface (Figure 1B). The median fluorescent intensity (MFI) of the GD2-bright population (defined by GD2 MFI of $>10^4$ based on the brightest point in the isotype staining – dotted line, Figure 2C) significantly increased for SK-N-AS shYAP1 (mean MFI = 44136) and SK-N-AS shYAP2 (mean MFI = 39032) following YAP knockdown compared to the SK-N-AS control (mean MFI = 2115) (Figure 2C,D). Additionally, the percentage of the GD2-bright cells was higher for SK-N-AS shYAP1 (mean = 30.2%) and SK-N-AS shYAP2 (mean = 38.7%) compared to the SK-NAS control (mean = 0.63%) (Figure 2E).

Given that YAP regulates chemotherapy response within the neuroblastoma TME and response to dinutuximab and γδ T cells *in vitro*, we ascertained whether YAP inhibition also influences tumor response to dinutuximab and γδ T cells *in vivo*.[16] We have previously shown that dinutuximab and γδ T cells are more effective against tumors *in vivo* with the addition of a cytotoxic agent, in keeping with clinical trials showing dinutuximab in combination with chemotherapy is more effective in patients with relapsed neuroblastoma compared to dinutuximab alone.[3,16,43] We treated NSG mice harboring established SK-N-AS control or shYAP subcutaneous tumors with dinutuximab, γδ T cells, and cyclophosphamide and monitored tumors for growth (Treatment schema, **Supplemental Figure S7A**). SK-N-AS shYAP tumors had a significant prolongation of tumor regression and survival

following treatment with dinutuximab, γδ T cells, and cyclophosphamide compared to mice with SK-N-AS control tumors ($p = 0.0024$) (**Supplemental Figure S7B**). We confirmed that YAP knockdown and lower expression of its canonical target, *CYR61*, were maintained in the SK-N-AS xenograft tumors at experimental endpoint after tumors recurred (**Supplemental Figure S7C and S7D**).

YAP inhibition increases cell surface expression of GD2 through upregulation of ST8SIA1

YAP can transcriptionally repress genes involved in therapy response.[13,16] Next-generation sequencing of paired diagnostic and relapsed high-risk neuroblastomas showed a significant decrease in expression of genes normally suppressed by YAP in relapsed tumors.[10] We therefore examined genes in the biosynthetic pathway of GD2 (Figure 3A), using RNA sequencing data from SK-N-AS control versus SK-N-AS shYAP1 cells.[16] *ST8SIA1*, which encodes for the critical rate-limiting enzyme GD3 synthase (GD3S) in the GD2 biosynthesis pathway, was found to be significantly increased (logFC = 2.62; $p = 5.87 \times 10^{-3}$) in SK-N-AS shYAP1 versus SK-N-AS control (Figure 3B). We validated this finding in both SK-N-AS shYAP1 and SK-N-AS shYAP2 models by RT-qPCR (Figure 3C). Reduced expression of *YAP* and its canonical target *CYR61* were confirmed in shYAP1 and shYAP2 cells compared to control and corresponded to significantly increased expression of *ST8SIA1* (>100-fold, $p < 0.01$) (Figure 3C). In the same models, other genes involved in the biosynthesis of GD2 (*B4GALT5/6*, *ST3GAL5*, *ST8SIA5*, *B4GALNT1*, *B3GALT4*, *ST3GAL2*) were either marginally changed or unchanged by RT-qPCR of shYAP1 and shYAP2 compared to control (**Supplemental Figure S8**). Notably, the gene encoding GD2 synthase (GD2S), *B4GALNT1*, was unchanged. Others have shown that forced expression of the master transcription factor *PRRX1* causes adrenergic-to-mesenchymal transition, leading to epigenetic suppression of genes like *ST8SIA1* in neuroblastoma.[44] Interestingly, the expression of *PRRX1* significantly increased with YAP knockdown for both SK-N-AS shYAP1 and shYAP2 compared to control, yet *ST8SIA1* expression and GD2 surface expression were not impacted (Figure 3C).

To confirm that GD2 cell surface changes were the result of YAP suppression of *ST8SIA1* (**Supplemental Figure S9**), we genetically inhibited *ST8SIA1* by shRNA in the SK-N-AS shYAP2 model. YAP knockdown was maintained in the control- and shST8SIA1-lentiviral transduced SK-N-AS shYAP2 cells (Figure 4A) and successful knockdown of *ST8SIA1* was achieved using two separate shST8SIA1 constructs (Figure 4B and Supplemental Figure S9). Genetic inhibition of *ST8SIA1* in the SK-N-AS shYAP2 cells led to significantly decreased median fluorescence intensity (MFI) of GD2 cell surface expression in SK-N-AS shYAP/shST8SIA1–1 and the SK-N-AS shYAP/shST8SIA1–2 compared to SK-N-AS shYAP/LV control, completely reversing the phenotype of increased GD2 surface expression upon YAP knockdown (Figure 4C,D). The percentage of GD2-positive cells in SK-N-AS shYAP shST8SIA1–1 and SK-N-AS shYAP shST8SIA1–2 was also >50-fold less than SK-N-AS shYAP control (Figure 4E). Furthermore, knockdown of *ST8SIA1* in SK-N-AS shYAP cells reduced their

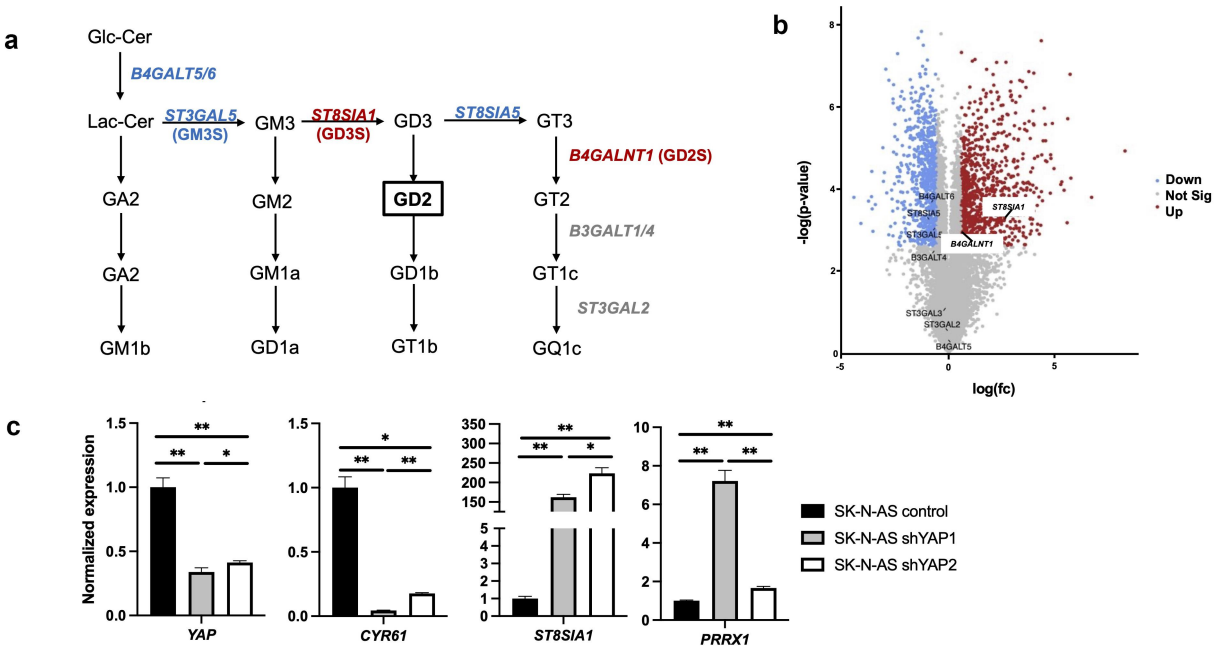

Figure 3. YAP inhibition mediates significantly increased gene expression of the GD2 biosynthetic enzyme, *ST8SIA1*. A, Schematic of ganglioside biosynthesis showing genes encoding enzymes in the biosynthetic pathway of GD2. Blue denotes genes downregulated, Red denotes genes upregulated, and Gray denotes genes unchanged in RNA sequencing data: SK-N-AS shYAP1 vs control. B, Volcano plot of -log(p-value) vs log(fold change(fc)) for GD2 biosynthetic genes from RNA seq data of SK-N-AS shYAP1 compared to control. Blue denotes genes downregulated, Red denotes genes upregulated, and Gray denotes genes not significantly changed. C, Normalized gene expression as determined by RT-qPCR of *YAP*: SK-N-AS control vs shYAP1: $^{**}p = 0.0011$, SK-N-AS control vs shYAP2: $^{**}p = 0.0040$, SK-N-AS shYAP1 vs shYAP2: $^{*}p = 0.0467$; YAP canonical target, *CYR61*: SK-N-AS control vs shYAP1: $^{**}p = 0.0078$, SK-N-AS control vs shYAP2: $^{*}p = 0.0102$, SK-N-AS shYAP1 vs shYAP2: $^{**}p = 0.0010$; *ST8SIA1*: SK-N-AS control vs shYAP1: $^{**}p = 0.0021$; SK-N-AS control vs shYAP2: $^{**}p = 0.0043$; SK-N-AS shYAP1 vs shYAP2: $^{*}p = 0.0349$; and *PRRX1*: SK-N-AS control vs shYAP1: $^{**}p = 0.0081$; SK-N-AS control vs shYAP2: $^{**}p = 0.0085$; SK-N-AS shYAP1 vs shYAP2: $^{**}p = 0.0091$. Data represent mean ± standard error of $n = 3$ independent experiments.

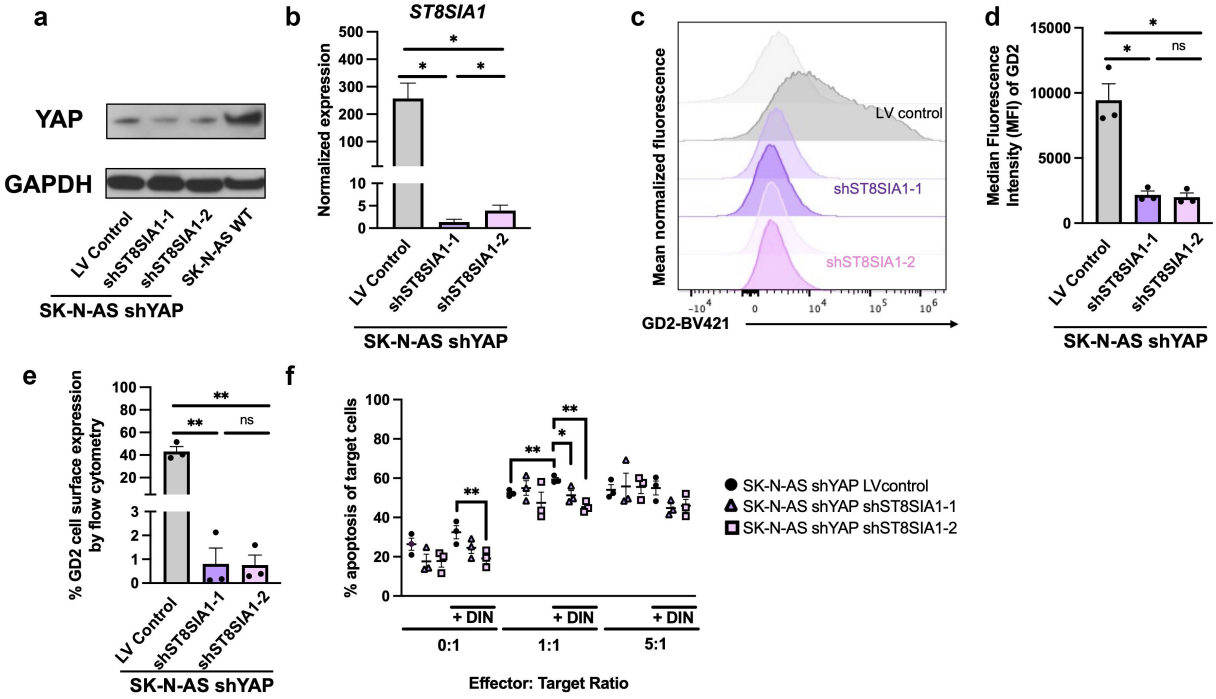

Figure 4. GD3S (*ST8SIA1*) inhibition reverses the phenotypes of increased GD2 surface expression and sensitivity to anti-GD2/γδ T cell immunotherapy when YAP is inhibited in SK-N-AS cells. A, Western blot of YAP expression in SK-N-AS shYAP lentiviral (LV) control, shYAP shST8SIA1–1, shYAP shST8SIA1–2, and SK-N-AS WT cells. GAPDH is the loading control. B, Normalized gene expression as determined by RT-Qpcr of *ST8SIA1* in dually transduced cells, SK-N-AS shYAP LV Control, SK-N-AS shYAP shST8SIA1–1, and SK-N-AS shYAP shST8SIA–2, SK-N-AS shYAP LV Control vs shYAP shST8SIA1–1: $*p = 0.0155$, SK-N-AS shYAP LV Control vs shYAP shST8SIA–2: $*p = 0.0157$, SK-N-AS shYAP shST8SIA1–1 vs shYAP shST8SIA–2: $*p = 0.0460$. C, Representative graph showing mean normalized fluorescence of GD2 cell surface expression by flow cytometry in SK-N-AS shYAP LV Control, SK-N-AS shYAP shST8SIA1–1, and SK-N-AS shYAP shST8SIA–2 cell lines. Lighter colors indicate isotype controls and darker colors indicate GD2-BV421 staining. D, Quantification of median fluorescence intensity (MFI) of GD2 in SK-N-AS shYAP LV Control, SK-N-AS shYAP shST8SIA1–1, and SK-N-AS shYAP shST8SIA–2 cell lines: SK-N-AS shYAP LV Control vs shYAP shST8SIA1–1: $*p = 0.0242$, SK-N-AS shYAP LV Control vs shYAP shST8SIA–2: $*p = 0.0221$. Data represent mean ± standard error of $n = 3$ independent experiments. E, Percentage of GD2 cell surface expression by flow cytometry in SK-N-AS shYAP LV Control, SK-N-AS shYAP shST8SIA1–1, SK-N-AS shYAP shST8SIA–2 cell lines; SK-N-AS shYAP LV Control vs shYAP LV shST8SIA1–1: $**p = 0.0088$, SK-N-AS shYAP LV Control vs shYAP shST8SIA–2: $**p = 0.0095$. Data represent mean ± standard error of $n = 3$ independent experiments. F, Percentage apoptosis of neuroblastoma target cells, SK-N-AS shYAP LV control, shYAP shST8SIA1–1, and shYAP shST8SIA1–2 when co-cultured for 4 hours with γδ T cells, with (+ DIN) and without dinutuximab, 0:1 +DIN: shYAP LV control vs shYAP shST8SIA1–2, $**p = 0.0056$; 1:1: shYAP LV control without DIN vs +DIN: $**p = 0.0076$; 1:1 +DIN: shYAP LV control vs shYAP shST8SIA1–1, $*p = 0.0392$; shYAP LV control vs shYAP shST8SIA1–2, $**p = 0.0018$; Data represent mean ± standard error of $n = 3$ independent experiments with two technical replicates per condition, student's T-test with Welch's correction. All other comparisons were not significant.

in vitro sensitivity to γδ T cells in the presence of dinutuximab compared to SK-N-AS shYAP/LV control, with no difference in neuroblastoma killing by γδ T cells in the absence of GD2-targeting antibody (Figure 4F).

YAP and ST8SIA1 or GD2 cell surface expression are inversely correlated in neuroblastoma primary tumors and patient derived xenografts

We queried publicly available gene expression datasets of primary neuroblastoma tumors to validate the clinical relevance of the regulation of GD2 by YAP through *ST8SIA1*. An inverse relationship between *YAP* and *ST8SIA1* expression was demonstrated in two separate datasets with non-overlapping cohorts: in the TARGET (Asgharzadeh) dataset, which consists of 249 samples assessed by exon array, R=-0.233, $p = 2.05\times10^{-4}$ (Figure 5A), and for the Kocak dataset, which consists of 648 samples assessed by microarray, R=-0.132, $p = 7.89\times10^{-4}$ (Figure 5B). Additionally, Kaplan–Meier survival analysis shows that the overall survival probability is reduced when *ST8SIA1* expression is lower (Figure 5C,D).

Since GD2 is a glycosphingolipid and thus, not genetically encoded, we sought to determine whether YAP protein expression and GD2 surface expression also inversely correlated by performing immunoblot and flow cytometry, respectively, in low-passage neuroblastoma patient-derived xenografts (PDXs). YAP expression was lower in NBx14r and NBx28r than in NBx27 and NBx34r (Figure 5E) and correspondingly, the MFI of GD2 on the surface of NBx14r and NBx28r was higher than that of NBx27 and NBx34r (Figure 5F).

Discussion

High-risk neuroblastomas that recur are notoriously chemotherapy resistant, leading to improvements in survival focused on immunotherapy approaches. Indeed, anti-GD2 antibodies in combination with chemotherapy have resulted in unprecedented response rates in relapsed patients.[22] However, challenges to GD2 targeted immunotherapies remain, such as an incomplete understanding of biomarkers predicting response and mechanisms of resistance.[30,31] High-risk neuroblastoma tumors that relapse are enriched with mesenchymal cells as well as RAS pathway mutations,[6,15,44] leading many to investigate how these properties may influence immunotherapy resistance to identify new therapeutic targets.

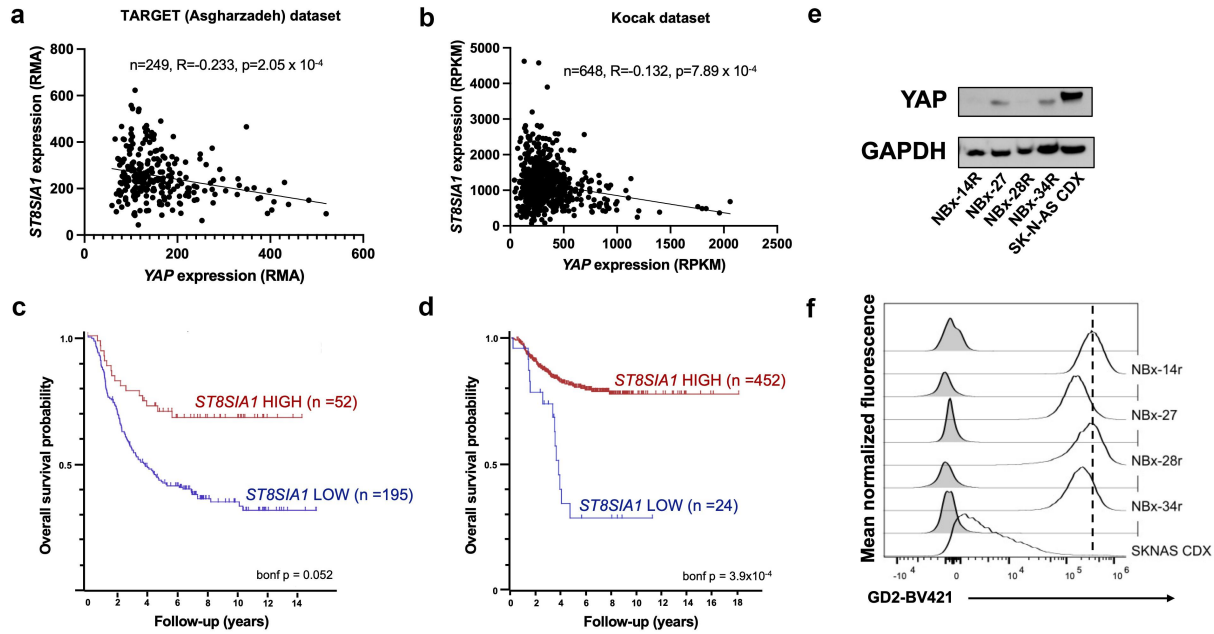

Figure 5. *YAP* and *ST8SIA1* expression are negatively correlated in primary neuroblastoma tumors, low *ST8SIA1* expression is associated with worse overall survival, and YAP and GD2 are inversely correlated in neuroblastoma patient derived xenografts (PDXs). *YAP* and *ST8SIA1* expression in primary neuroblastoma tumors from patients: A, TARGET (Asghardazeh) dataset: n = 249, *R*=-0.233, p = 2.05 × 10^{-4}. B, Kocak dataset: n = 648, *R*=-0.132, p = 7.89 × 10^{-4}. Low *ST8SIA1* expression in primary neuroblastoma tumors from patients is associated with worse overall survival: C, TARGET (Asghardazeh) dataset: n = 247, Bonferroni-corrected (bonf.) p = 0.052. D, Kocak dataset: n = 476, *R*=-0.137, bonf. p = 3.9 × 10^{-4}. https://r2.amc.nl. E, Western blot of YAP expression in neuroblastoma patient-derived xenografts (PDXs), NBx-14r, NBx-27, NBx-28r, NBx-34r and the SK-N-AS neuroblastoma cell line-derived xenograft (CDX). GAPDH is the loading control. F, Mean normalized fluorescence of GD2 cell surface expression by flow cytometry in neuroblastoma patient-derived xenografts (PDXs), NBx-14r, NBx-27, NBx-28r, NBx-34r and the SK-N-AS neuroblastoma cell line-derived xenograft (CDX). Grey denotes isotype control staining and white denotes GD2-BV421 staining.

YAP is a canonical mesenchymal gene that encodes for the YAP protein known to cooperate with hyperactivated RAS.[17] Indeed, the YAP expressing neuroblastoma cell lines we investigated are RAS pathway mutated (SK-N-AS, NLF) and harbor the mesenchymal gene signature.[15,44,45] Our findings demonstrate that *YAP* genetic inhibition paradoxically leads to upregulated expression of *PRRX1*, one of the master transcription factors that can drive the mesenchymal phenotype.[44] Previously, it was shown that genetic induction of mesenchymal neuroblastoma via overexpression of *PRRX1* induces similar transcriptional downregulation of *ST8SIA1* with resultant decrease of cell surface GD2.[31] PRRX1 converts an adrenergic neuroblastoma cell to a mesenchymal neuroblastoma cell (adrenergic to mesenchymal transition) with a decrease in adrenergic-differentiating genes like *PHOX2B*, *GATA2*, *DLK1* and an increase in mesenchymal stem-like genes such as *SOX2*, *SNAI2* and *YAP*.[44] We now show that YAP is sufficient to suppress the same glycosphingolipid biosynthesis pathway regardless of *PRRX1* gene expression, suggesting that GD2 synthesis may be more directly regulated by YAP downstream of its mesenchymal driving forces such as PRRX1 and other master mesenchymal transcription factors. Further studies are warranted to validate the full functional roles for YAP within the mesenchymal neuroblastoma phenotype.

Despite the success of dinutuximab and other anti-GD2 antibodies, not all patients respond, and preclinical data suggest that it may be due to lack of GD2 on the tumor cell surface. Detection of GD2 in primary neuroblastoma tissue is limited since GD2 is a glycosphingolipid and its presence is therefore not detectable by immunohistochemistry on paraffin embedded tissue.[18] Recent studies have therefore sought to determine and provide surrogate biomarkers for GD2 expression in an effort to triage patients most likely to benefit from GD2 immunotherapy.[31] We found that neuroblastomas with low GD2 have high YAP gene and protein expression. Furthermore, this inverse correlation has functional relevance as we found YAP to suppress GD2 expression through inhibition of the GD3 synthase (GD3S) gene *ST8SIA1*. By suppressing GD3S and thus GD2 synthesis, YAP indeed serves as a mediator and potential biomarker of anti-GD2 antibody resistance. We validated this relationship through genetic knockdown studies, showing YAP inhibition restores response to dinutuximab and γδ T cells both *in vitro* and *in vivo* in SK-N-AS, with the therapy resistant phenotype restored upon knockdown of *ST8SIA1* in the shYAP neuroblastoma cells. We also observed a trend toward inverse correlation between YAP protein and GD2 cell surface expression in low-passage high risk and relapsed neuroblastoma PDXs. In addition, primary neuroblastomas also show an inverse correlation between genetic expression of *YAP* and *ST8SIA1*. Based on these data, we hypothesize that high YAP expression in neuroblastoma tumors may predict GD2 immunotherapy resistance clinically. Immunohistochemical staining of YAP in primary neuroblastoma tumors is feasible and should be characterized prospectively to statistically correlate results to patient outcomes following anti-GD2 therapy to concretely define it as a biomarker of response.

A slight increase in neuroblastoma cell death was observed following coculture with γδ T cells alone in the SK-N-AS shYAP cells compared to control. We therefore investigated whether increased tumor cell death was due to paracrine effects of the YAP-inhibited neuroblastoma cells toward the γδ T cells.

When SK-N-AS shYAP cells were co-cultured with γδ T cells, we observed no difference in γδ T cell markers of exhaustion, activation, or apoptosis, nor an increase in tumor-resident stress antigens or FAS/TRAIL receptors. Although there was an increase in IFNγ release when SK-N-AS shYAP cells were treated with the combination of γδ T cells and dinutuximab *in vitro*, this increased IFNγ release was not consistently observed in the absence of dinutuximab. This suggests that differences in cytotoxicity were not due to γδ T cell-intrinsic changes, increased release of cytotoxic mediators, or by increased T cell recognition ligands on the tumor cells. Further investigation is warranted to understand the effect of tumor YAP inhibition on increased γδ T cell activity.

YAP expression by immune cells themselves has been shown to promote immunosuppression and suppress immunotherapy activity.[46] For example, high YAP expression in regulatory T cells of hepatocellular carcinoma patients was found to facilitate an immunosuppressive TME and was an indicator of poor prognosis.[47] Since YAP has a well-established role in the TME, its role in the neuroblastoma TME-enacted resistance to anti-GD2 immunotherapy warrants evaluation by using immunocompetent murine models. Indeed, future studies in additional neuroblastoma models will identify whether therapeutic targeting of YAP may be beneficial by not only making tumor cells more vulnerable through upregulation of the immunotherapy target, but also through inhibition of immune cells contributing to the immune hostile TME.

Others have identified that mesenchymal master transcription factors epigenetically suppress *ST8SIA1* expression, leading clinical efforts to evaluate the combination of GD2 antibodies with epigenetic modifying agents such as EZH2 inhibitors (tazemetostat) and the histone deacetylase inhibitor, vorinostat.[31,48] These epigenetic approaches to increase GD2 surface expression may be viable for improving targeting neuroblastoma cell populations that express low cell surface GD2 ($GD2^{low}$) in patients. Additionally, dual targeting of other highly expressed neuroblastoma antigens like B7-H3 or GPC2 with GD2 could ensure tumor specificity and optimize the targeting of $GD2^{low}$ neuroblastoma.[49–51] Here, we demonstrate increased *ST8SIA1* expression in SK-N-AS neuroblastoma cells upon genetic inhibition of YAP and an inverse relationship between *YAP* and *ST8SIA1* in primary neuroblastoma tumors. Further mechanistic studies in additional models will be important to confirm our findings and determine the mechanism by which YAP suppresses *ST8SIA1*. If confirmed, these studies would lay the foundation for combining targeted YAP inhibition as a way to sensitize $GD2^{low}$ neuroblastomas to anti-GD2 immunotherapy similar to epigenetic-modifying agents.

Overall, our findings have defined a role for YAP in down-regulation of *ST8SIA1*, rendering GD2 antibody resistance in neuroblastoma cell lines. These results support that both *ST8SIA1* (GD3 synthase) and YAP warrant further investigation with regard to their expression in relation to clinical response to anti-GD2 antibody immunotherapy. Currently, inhibitors of the YAP/TEAD interaction have shown preclinical promise in adult cancers with one agent in clinical application for adult mesothelioma,[52] and investigations are ongoing to evaluate such inhibitors in neuroblastoma. Incorporation of YAP pharmacological inhibition with novel GD2 targeting immunotherapies, such as GD2-CAR T cells or novel anti-GD2 antibody combinations (γδ T cells with dinutuximab and chemotherapy; NCT05400603) may also improve outcomes for patients with high-risk and relapsed neuroblastoma.[53]

Acknowledgments

We thank the Children's Healthcare of Atlanta and Emory University's Pediatric Flow Cytometry Core for support with flow cytometry experiments.

Disclosure statement

No potential conflict of interest was reported by the authors.

Funding

This work was supported by the CURE Childhood Cancer Foundation to KCG and Atlanta Pediatric Scholars Program K12 Scholar supported by the National Institutes of Health, Eunice Kennedy Shriver National Institute of Child Health and Human Development grant K12HD072245 to JS.

Data availability statement

The data that support the findings of this study are available from the corresponding author, KCG, upon reasonable request.

References

1. Matthay KK, Maris JM, Schleiermacher G, Nakagawara A, Mackall CL, Diller L, Weiss WA. Neuroblastoma. Nat Rev Dis Primers. 2016 Nov 10;2(1):16078. doi:10.1038/nrdp.2016.78.
2. London WB, Bagatell R, Weigel BJ, et al. Historical time to disease progression and progression-free survival in patients with recurrent/refractory neuroblastoma treated in the modern era on children's oncology group early-phase trials. Cancer. 2017 Dec 15;123 (24):4914–4923. doi:10.1002/cncr.30934.
3. Mody R, Yu AL, Naranjo A, Zhang FF, London WB, Shulkin BL, Parisi MT, Servaes SEN, Diccianni MB, Hank JA, et al. Irinotecan, temozolomide, and dinutuximab with GM-CSF in children with refractory or relapsed neuroblastoma: a report from the children's oncology group. J Clin Oncol. 2020 01 07;38(19):2160–2169. doi:10.1200/JCO.20.00203.
4. Lerman BJ, Li Y, Carlowicz C, Granger M, Cash T, Sadanand A, Somers K, Ranavaya A, Weiss BD, Choe M, et al. Progression-free survival and patterns of response in patients with relapsed high-risk neuroblastoma treated with irinotecan/temozolomide/dinutuximab/granulocyte-macrophage colony-stimulating factor. J Clin Oncol. 2023 Jan 20;41(3):508–516. doi:10.1200/JCO.22.01273.
5. Chen L, Humphreys A, Turnbull L, Bellini A, Schleiermacher G, Salwen H, Cohn SL, Bown N, Tweddle DA. Identification of different ALK mutations in a pair of neuroblastoma cell lines established at diagnosis and relapse. Oncotarget. 2016 Dec 27;7 (52):87301–87311. doi:10.18632/oncotarget.13541.
6. Eleveld TF, Oldridge DA, Bernard V, Koster J, Daage LC, Diskin SJ, Schild L, Bentahar NB, Bellini A, Chicard M, et al. Relapsed neuroblastomas show frequent RAS-MAPK pathway mutations. Nat Genet. 2015 08;47(8):864–871. doi:10.1038/ng.3333.
7. Padovan-Merhar OM, Raman P, Ostrovnaya I, Kalletla K, Rubnitz KR, Sanford EM, Ali SM, Miller VA, Mossé YP, Granger MP, et al. Enrichment of targetable mutations in the

relapsed neuroblastoma genome. PLoS Genet. 2016 Dec;12(12): e1006501. doi:10.1371/journal.pgen.1006501.
8. Schulte M, Köster J, Rahmann S, Schramm A. Cancer evolution, mutations, and clonal selection in relapse neuroblastoma. Cell Tissue Res. 2018 May;372(2):263–268. doi:10.1007/s00441-018-2810-5.
9. Schleiermacher G, Javanmardi N, Bernard V, Leroy Q, Cappo J, Rio Frio T, Pierron G, Lapouble E, Combaret V, Speleman F, et al. Emergence of new ALK mutations at relapse of neuroblastoma. J Clin Oncol. 2014 Sep 1;32(25):2727–2734. doi:10.1200/JCO.2013.54.0674.
10. Schramm A, Köster J, Assenov Y, Althoff K, Peifer M, Mahlow E, Odersky A, Beisser D, Ernst C, Henssen AG, et al. Mutational dynamics between primary and relapse neuroblastomas. Nat Genet. 2015 Aug;47(8):872–877. doi:10.1038/ng.3349.
11. Vassilev A, Kaneko KJ, Shu H, Zhao Y, DePamphilis ML. TEAD/TEF transcription factors utilize the activation domain of YAP65, a Src/Yes-associated protein localized in the cytoplasm. Genes Dev. 2001 May 15;15(10):1229–1241. doi:10.1101/gad.888601.
12. Yagi R, Chen LF, Shigesada K, Murakami Y, Ito Y. A WW domain-containing yes-associated protein (YAP) is a novel transcriptional co-activator. Embo J. 1999 May 4;18(9):2551–2562. doi:10.1093/emboj/18.9.2551.
13. Kim M, Kim T, Johnson RL, Lim DS. Transcriptional co-repressor function of the hippo pathway transducers YAP and TAZ. Cell Rep. 2015 Apr 14;11(2):270–282. doi:10.1016/j.celrep.2015.03.015.
14. Ahmed AA, Mohamed AD, Gener M, Li W, Taboada E. YAP and the hippo pathway in pediatric cancer. Mol Cell Oncol. 2017;4(3): e1295127. doi:10.1080/23723556.2017.1295127.
15. Boeva V, Louis-Brennetot C, Peltier A, Durand S, Pierre-Eugène C, Raynal V, Etchevers HC, Thomas S, Lermine A, Daudigeos-Dubus E, et al. Heterogeneity of neuroblastoma cell identity defined by transcriptional circuitries. Nat Genet. 2017 Sep;49(9):1408–1413. doi:10.1038/ng.3921.
16. Shim J, Lee JY, Jonus HC, Arnold A, Schnepp RW, Janssen KM, Maximov V, Goldsmith KC. YAP-mediated repression of HRK regulates tumor growth, therapy response, and survival under tumor environmental stress in neuroblastoma. Cancer Res. 2020 11;80(21):4741–4753. doi:10.1158/0008-5472.CAN-20-0025.
17. Coggins GE, Farrel A, Rathi KS, Hayes CM, Scolaro L, Rokita JL, Maris JM. YAP1 mediates resistance to MEK1/2 inhibition in neuroblastomas with hyperactivated RAS signaling. Cancer Res. 2019 12-15;79(24):6204–6214. doi:10.1158/0008-5472.CAN-19-1415.
18. Wu ZL, Schwartz E, Seeger R, Ladisch S. Expression of GD2 ganglioside by untreated primary human neuroblastomas. Cancer Res. 1986 Jan;46(1):440–443.
19. Ladisch S, Wu ZL. Detection of a tumour-associated ganglioside in plasma of patients with neuroblastoma. Lancet. 1985 Jan 19;1 (8421):136–138. doi:10.1016/s0140-6736(85)91906-3.
20. Sariola H, Harri T, Rapola J, Saarinen UM. Cell-surface ganglioside GD2 in the immunohistochemical detection and differential diagnosis of neuroblastoma. Am J Clin Pathol. 1991 Aug;96 (2):248–252. doi:10.1093/ajcp/96.2.248.
21. Mujoo K, Cheresh DA, Yang HM, Reisfeld RA. Disialoganglioside GD2 on human neuroblastoma cells: target antigen for monoclonal antibody-mediated cytolysis and suppression of tumor growth. Cancer Res. 1987 Feb 15;47(4):1098–1104.
22. Yu AL, Gilman AL, Ozkaynak MF, London WB, Kreissman SG, Chen HX, Smith M, Anderson B, Villablanca JG, Matthay KK, et al. Anti-GD2 antibody with GM-CSF, interleukin-2, and isotretinoin for neuroblastoma. N Engl J Med. 2010 Sep 30;363(14):1324–1334. doi:10.1056/NEJMoa0911123.
23. Yu AL, Gilman AL, Ozkaynak MF, Naranjo A, Diccianni MB, Gan J, Hank JA, Batova A, London WB, Tenney SC, et al. Long-term follow-up of a phase III study of ch14.18 (dinutuximab) + cytokine immunotherapy in children with high-risk neuroblastoma: COG study ANBL0032. Clin Cancer Res. 2021 04 15;27 (8):2179–2189. doi:10.1158/1078-0432.CCR-20-3909.
24. Kushner BH, Cheung IY, Modak S, Basu EM, Roberts SS, Cheung NK. Humanized 3F8 Anti-GD2 monoclonal antibody dosing with granulocyte-macrophage colony-stimulating factor in patients with resistant neuroblastoma: a phase 1 clinical trial. JAMA Oncol. 2018 Dec 01;4(12):1729–1735. doi:10.1001/jamaoncol.2018.4005.
25. Blom T, Lurvink R, Aleven L, Mensink M, Wolfs T, Dierselhuis M, van Eijkelenburg N, Kraal K, van Noesel M, van Grotel M, et al. Treatment-related toxicities during anti-GD2 immunotherapy in high-risk neuroblastoma patients. Front Oncol. 2020;10:601076. doi:10.3389/fonc.2020.601076.
26. Ozkaynak MF, Gilman AL, London WB, Naranjo A, Diccianni MB, Tenney SC, Smith M, Messer KS, Seeger R, Reynolds CP, et al. A Comprehensive safety trial of chimeric antibody 14.18 with GM-CSF, IL-2, and isotretinoin in high-risk neuroblastoma patients following myeloablative therapy: children's oncology group study ANBL0931. Front Immunol. 2018;9:1355. doi:10.3389/fimmu.2018.01355.
27. Majzner RG, Mackall CL. Tumor antigen escape from CAR T-cell therapy. Cancer Discov. 2018 Oct;8(10):1219–1226. doi:10.1158/2159-8290.CD-18-0442.
28. Terzic T, Cordeau M, Herblot S, Teira P, Cournoyer S, Beaunoyer M, Peuchmaur M, Duval M, Sartelet H. Expression of disialoganglioside (GD2) in neuroblastic tumors: a prognostic value for patients treated with anti-GD2 immunotherapy. Pediatr Dev Pathol. 2018;21(4):355–362. doi:10.1177/1093526617723972.
29. Schumacher-Kuckelkorn R, Volland R, Gradehandt A, Hero B, Simon T, Berthold F. Lack of immunocytological GD2 expression on neuroblastoma cells in bone marrow at diagnosis, during treatment, and at recurrence. Pediatr Blood Cancer. 2017 Jan;64 (1):46–56. doi:10.1002/pbc.26184.
30. Schumacher-Kuckelkorn R, Hero B, Ernestus K, Berthold F. Lacking immunocytological GD2 expression in neuroblastoma: report of 3 cases. Pediatr Blood Cancer. 2005 Aug;45(2):195–201. doi:10.1002/pbc.20301.
31. Mabe NW, Huang M, Dalton GN, Alexe G, Schaefer DA, Geraghty AC, Robichaud AL, Conway AS, Khalid D, Mader MM, et al. Transition to a mesenchymal state in neuroblastoma confers resistance to anti-GD2 antibody via reduced expression of ST8SIA1. Nat Cancer. 2022 Jul 11;3(8):976–993. doi:10.1038/s43018-022-00405-x.
32. Jonus HC, Burnham RE, Ho A, Pilgrim AA, Shim J, Doering CB, Spencer HT, Goldsmith KC. Dissecting the cellular components of ex vivo γδ T cell expansions to optimize selection of potent cell therapy donors for neuroblastoma immunotherapy trials. Oncoimmunol. 2022;11(1):2057012. doi:10.1080/2162402X.2022.2057012.
33. Zoine JT, Knight KA, Fleischer LC, Sutton KS, Goldsmith KC, Doering CB, Spencer HT. Ex vivo expanded patient-derived γδ T-cell immunotherapy enhances neuroblastoma tumor regression in a murine model. Oncoimmunol. 2019;8(8):1593804. doi:10.1080/2162402X.2019.1593804.
34. Mensurado S, Blanco-Domínguez R, Silva-Santos B. The emerging roles of γδ T cells in cancer immunotherapy. Nat Rev Clin Oncol. 2023 Jan 09. doi:10.1038/s41571-022-00722-1.
35. Alter G, Malenfant JM, Altfeld M. Cd107a as a functional marker for the identification of natural killer cell activity. J Immunol Methods. 2004 Nov;294(1–2):15–22. doi:10.1016/j.jim.2004.08.008.
36. Rubio V, Stuge TB, Singh N, Betts MR, Weber JS, Roederer M, Lee PP. Ex vivo identification, isolation and analysis of tumor-cytolytic T cells. Nat Med. 2003 Nov;9(11):1377–1382. doi:10.1038/nm942.
37. Betts MR, Brenchley JM, Price DA, De Rosa SC, Douek DC, Roederer M, Koup RA. Sensitive and viable identification of antigen-specific CD8+ T cells by a flow cytometric assay for degranulation. Jf Immunol Meth. 2003 Oct 01;281(1–2):65–78. doi:10.1016/s0022-1759(03)00265-5.
38. Vantourout P, Hayday A. Six-of-the-best: unique contributions of γδ T cells to immunology. Nat Rev Immunol. 2013 Feb;13 (2):88–100. doi:10.1038/nri3384.

39. Silva-Santos B, Mensurado S, Coffelt SB. γδ T cells: pleiotropic immune effectors with therapeutic potential in cancer. Nat Rev Cancer. 2019 07;19(7):392–404. doi:10.1038/s41568-019-0153-5.
40. Gao Y, Yang W, Pan M, Scully E, Girardi M, Augenlicht LH, Craft J, Yin Z. γδ T cells provide an early source of interferon γ in tumor immunity. J Experiment Med. 2003 Aug 04;198 (3):433–442. doi:10.1084/jem.20030584.
41. Zhang R, Banik NL, Ray SK. Combination of all-trans retinoic acid and interferon-gamma suppressed PI3K/Akt survival pathway in glioblastoma T98G cells whereas NF-kappaB survival signaling in glioblastoma U87MG cells for induction of apoptosis. Neurochem Res. 2007 Dec;32(12):2194–2202. doi:10.1007/s11064-007-9417-7.
42. George RE, Sanda T, Hanna M, Fröhling S, Ii WL, Zhang J, Ahn Y, Zhou W, London WB, McGrady P, et al. Activating mutations in ALK provide a therapeutic target in neuroblastoma. Nature. 2008 Oct 16;455(7215):975–978. doi:10.1038/nature07397.
43. Gilman AL, Ozkaynak MF, Matthay KK, Krailo M, Yu AL, Gan J, Sternberg A, Hank JA, Seeger R, Reaman GH, et al. Phase I study of ch14.18 with granulocyte-macrophage colony-stimulating factor and interleukin-2 in children with neuroblastoma after autologous bone marrow transplantation or stem-cell rescue: a report from the children's oncology group. J Clin Oncol. 2009 Jan 1;27(1):85–91. doi:10.1200/JCO.2006.10.3564.
44. van Groningen T, Koster J, Valentijn LJ, Zwijnenburg DA, Akogul N, Hasselt NE, Broekmans M, Haneveld F, Nowakowska NE, Bras J, et al. Neuroblastoma is composed of two super-enhancer-associated differentiation states. Nat Genet. 2017 Aug;49(8):1261–1266. doi:10.1038/ng.3899.
45. Stokes ME, Small JC, Vasciaveo A, Shimada K, Hirschhorn T, Califano A, Stockwell BR. Mesenchymal subtype neuroblastomas are addicted to TGF-βR2/HMGCR-driven protein geranylgeranylation. Sci Rep. 2020 Jul 01;10(1):10748. doi:10.1038/s41598-020-67310-0.
46. Stampouloglou E, Cheng N, Federico A, Slaby E, Monti S, Szeto GL, Varelas X. Yap suppresses T-cell function and infiltration in the tumor microenvironment. PLoS Biol. 2020 Jan;18(1): e3000591. doi:10.1371/journal.pbio.3000591.
47. Fan Y, Gao Y, Rao J, Wang K, Zhang F, Zhang C. YAP-1 promotes tregs differentiation in hepatocellular carcinoma by enhancing TGFBR2 transcription. Cell Physiol Biochem. 2017;41 (3):1189–1198. doi:10.1159/000464380.
48. van den Bijgaart RJE, Kroesen M, Brok IC, Reijnen D, Wassink M, Boon L, Hoogerbrugge PM, Adema GJ. Anti-GD2 antibody and vorinostat immunocombination therapy is highly effective in an aggressive orthotopic neuroblastoma model. Oncoimmunol. 2020 09-20;9(1):1817653. doi:10.1080/2162402X.2020.1817653.
49. Dondero A, Morini M, Cangelosi D, Mazzocco K, Serra M, Spaggiari GM, Rotta G, Tondo A, Locatelli F, Castellano A, et al. Multiparametric flow cytometry highlights B7-H3 as a novel diagnostic/therapeutic target in GD2neg/low neuroblastoma variants. J Immunother Cancer. 2021 04;9(4):e002293. doi:10.1136/jitc-2020-002293.
50. Moghimi B, Muthugounder S, Jambon S, Tibbetts R, Hung L, Bassiri H, Hogarty MD, Barrett DM, Shimada H, Asgharzadeh S, et al. Preclinical assessment of the efficacy and specificity of GD2-B7H3 SynNotch CAR-T in metastatic neuroblastoma. Nat Commun. 2021 Jan 21;12(1):511. doi:10.1038/s41467-020-20785-x.
51. Bosse KR, Raman P, Zhu Z, Lane M, Martinez D, Heitzeneder S, Rathi KS, Kendsersky NM, Randall M, Donovan L, et al. Identification of GPC2 as an oncoprotein and candidate immunotherapeutic target in high-risk neuroblastoma. Cancer Cell. 2017 Sep 11;32(3):295–309.e12. doi:10.1016/j.ccell.2017.08.003.
52. Tang TT, Konradi AW, Feng Y, Peng X, Ma M, Li J, Yu F-X, Guan KL, Post L. Small molecule inhibitors of TEAD auto-palmitoylation selectively inhibit proliferation and tumor growth of NF2-deficient mesothelioma. Mol Cancer Ther. 2021 Jun;20(6):986–998. doi:10.1158/1535-7163.MCT-20-0717.
53. Del Bufalo F, De Angelis B, Caruana I, Del Baldo G, De Ioris MA, Serra A, Mastronuzzi A, Cefalo MG, Pagliara D, Amicucci M, et al. GD2-CART01 for relapsed or refractory high-risk neuroblastoma. N Engl J Med. 2023 Apr 6;388(14):1284–1295. doi:10.1056/NEJMoa2210859.